HIGH SPEED FLUTTERING SKIDS WITH ELASTIC SUSPENSIONS

Gianluca Pepe, Antonio Carcaterra

Department of Mechanical and Aerospace Engineering, Sapienza University of Rome, Italy
E-mail: gianluca.pepe@uniroma1.it, a.carcaterra@dma.ing.uniroma1.it

ABSTRACT

In a recent project, named SEALAB, a novel marine vehicle has been developed. Its main characteristic is the presence of special skid surfaces surfing over rough water. A suspension system controls the vertical motion of the skid, softening the sequential impacts and vibrations induced by the water, similarly to a wheeled vehicle in off-road trials. The hull-skid-suspension set is modeled by prototypical equations. The system undergoes special regimes when the vessel speed at sea is varied. In particular, for some combinations of the forward speed and sea-state, the skid still maintains the contact with the water. In other navigation conditions the skid indeed jumps out the water with a complete different average transmitted force and vibration characteristics of the hull. This paper presents a theory that outlines these phenomena identifying conditions that lead to the jumping skid condition.

1. INTRODUCTION

SEALAB is a recent project aimed at developing an innovative high-speed marine vehicle. This new concept vehicle navigates at high speed in sea waves as a aero-hydro-foils with a set of skids, connected to a sophisticated smart suspension link (Carcaterra, Scorrano, & Pepe, SEALAB: Aero-hydro mechanics of a three-wings jumping vehicle, 2011).
Its design poses new problems related to the phenomenology of the high speed fluttering skids.

Figure 1: SEALAB model design, rendering of external structures

The capability of the vehicle relies in keeping the trim and stability at high speed when jumping on rough sea. A statistical mathematical model describing the navigation mechanics is developed based on a two-degrees-of-freedom system, in which the skid-water interaction plays a crucial role. The model permits to disclose two different navigation conditions: at low speed,

and given the sea state, the skid still maintains a continuous contact with the water; at high speed the skid undergoes indeed large vertical displacements that produce its water exit leading to an intermittent contact with the sea surface, with the typical jumping navigation condition. In particular, the paper identifies a critical speed, depending on the sea-state and the vehicle speed at which the transition between the continuous and the intermittent contact between skid and water surface is observed.

2. PROTOTIPYCAL EQUATIONS OF THE FLUTTERING SKID

In its simplest modeling, the vehicle is idealized as a two-mass model. The upper one is associated to the hull and the second one to the surfing skid. The skid, in the real vehicle, is attached to the hull through a rather sophisticated suspension system including also semi-active controls and special kinematic linkages, here idealized by a simply sprung skid. Additionally, the real vehicle is equipped with air-hydrofoils that partially cooperate to the lift and mainly to the vehicle trim keeping.
The navigation of the innovative vessel follows different navigation regimes, depending on its operating speed and on the encountered sea state. The vessel, at low speed, behaves as a displacement ship then, increasing its speed, a planning-hull behavior is observed, followed by the hull water exit lifted essentially by the skid hydrodynamic force with contributions of the other air-hydrofoils. The present model assumes the whole hull lifting action is provided by the skid hydrodynamic force. The chance of reaching very high speed, even for rough sea, is assured by the skid action that provides (i) the lifting force avoiding the direct water-hull contact, (ii) the mitigation of the forces transmitted to the hull by the skid strut due to the interposition of a suspension element, (iii) the intermittent loss of contact between water and skid when a critical speed is reached, allowing to jump over the waves crests reducing the heave oscillations, the vehicle center of mass trajectory following a sort of wave envelope.
The general model of the system comprises the equation of motion for the vessel, coupled to the equation of motion of the skid:

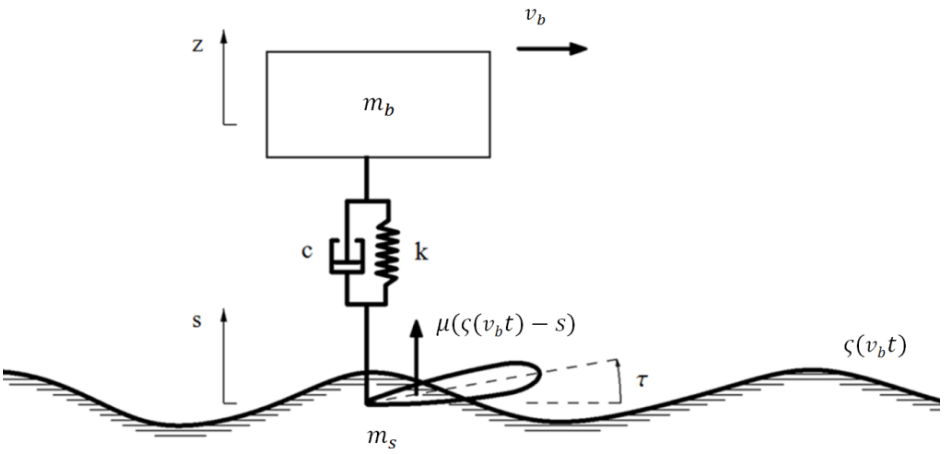

Figure 2: Model with two degrees of freedom

$$\begin{cases} \ddot{z}m_b - c\dot{s} + c\dot{z} - ks + kz = 0 \\ \ddot{s}m_s - c\dot{z} + c\dot{s} - kz + ks = L_{Skid}(s, \varsigma(v_b t)) \end{cases} \tag{1}$$

where m_b, m_s, k, c, $z(t)$, $s(t)$, v_b, $\varsigma(v_b t)$ are the boat and skid masses, the stiffness and damping of the suspension system, the absolute heave motion of the hull (z) and of the skid (s),the forward speed of the boat, and the water surface elevation (with respect to the reference plane for still water), respectively. This last quantity is a random variable controlled by known statistics (e.g. Pearson-Moskowitz, Jonswap).

2.1 Linearization the lift force of the skid

Assuming for the skid hydrodynamic force the usual representation making use of the lift coefficient, the equation of motion become:

$$\begin{cases} \ddot{z}m_b - c\dot{s} + c\dot{z} - ks + kz = 0 \\ \ddot{s}m_s - c\dot{z} + c\dot{s} - kz + ks = \frac{1}{2}\rho {v_b}^2 \mathcal{S}_{wet}(s) c_L(s) \end{cases} \tag{2}$$

and

$$L_{Skid} = \frac{1}{2}\rho S_{wet} {v_b}^2 c_L \tag{3}$$

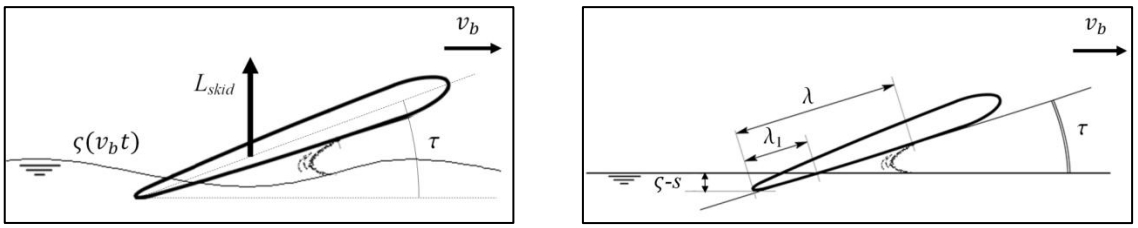

Figure 3: Schematization of the skid

The skid trim angle is τ (degrees), $S_{wet} = bc_{wet}$ is the wetted surface of the skid, b is the wingspan, c_{wet} the wetted chord. As a first approximation we can consider the wetted chord as $c_{wet} = \frac{\varsigma(v_b t) - s}{sen\left(\frac{\pi\tau}{180}\right)}$. Thus, equation (3) produces:

$$L_{Skid} = \frac{1}{2}\rho b \frac{\varsigma(v_b t) - s}{sen\left(\frac{\pi\tau}{180}\right)} {v_b}^2 c_L(s) \tag{4}$$

The lift coefficient c_L can be assumed to be (Savitsky, 1964):

$$c_L = \tau^{1,1}\left[0.012\sqrt{\lambda} + \frac{0.0055\lambda^{5/2}}{Fr^2}\right] \tag{5}$$

where $Fr = \frac{v_b}{\sqrt{gb}}$. Two nondimensional parameters, λ_1 and λ are introduced; the first $\lambda_1 = \frac{c_{wet}}{b}$ is the nondimensional wetted length based on purely geometric factors, the second is the corrected wetted length considering the water surface deformation due to the spray effect. The second can be expressed in terms of the first using the empirical correlations:

$$\begin{cases} \lambda = 1{,}6\lambda_1 - 0{,}3{\lambda_1}^2 & for \quad 0 \le \lambda_1 \le 1 \\ \lambda = \lambda_1 + 0{,}3 & for \quad 1 \le \lambda_1 \le 4 \quad \text{(skid model)} \end{cases} \tag{6}$$

The lift coefficient c_L can be expressed by equation (5) under the restrictions for τ, λ and Fr:

$$2° \le \tau \le 15° \tag{7}$$

$$\lambda \le 4 \tag{8}$$

$$0{,}6 \le \mathrm{Fr} \le 13 \tag{9}$$

Figure 4 shows L_{Skid} dependence on the trailing edge depth of the skid Δ, we can confirm that the case called $skid\ model\ \ \lambda = \lambda_1 + 0{,}3\ for\ 1 \le \lambda_1 \le 4$ approximate well the first case $\lambda = 1{,}6\lambda_1 - 0{,}3{\lambda_1}^2\ for\ 0 \le \lambda_1 \le 1$.

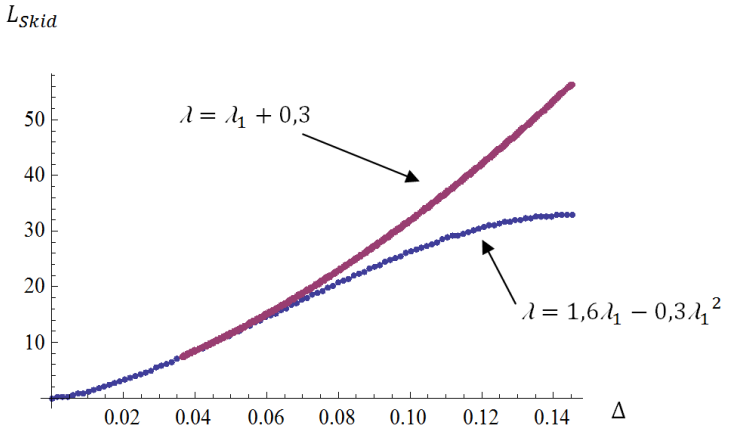

Figure 4: Skid lift vs skid trailing edge depth, for $\tau = 14°, v_b = 14\,{}^{m}/_{s}\,, b = 0{,}15m$

Note the limitation $\lambda \leq 4$ implies the depth restriciton:

$$\Delta_{MAX} \leq 3{,}7 * b * \sin\frac{\pi\tau}{180} \tag{10}$$

and the Froude number limits $0{,}6 \leq \mathrm{Fr} \leq 13$ produce:

$$\begin{cases} v_{b_{Max}} = 13\sqrt{gb} \\ v_{b_{Min}} = 0{,}6\sqrt{gb} \end{cases} \tag{11}$$

The Savitsky's lift coefficient c_L with $\lambda_1 = \frac{C_{wet}}{b} = \frac{\varsigma(v_b t)-s}{b\,sen\left(\frac{\pi\tau}{180}\right)}$ becomes:

$$c_L = \tau^{1{,}1}\left[0.012\sqrt{\frac{\varsigma(v_b t)-s}{b\,sen\left(\frac{\pi\tau}{180}\right)}} + 0{,}3 + \frac{0.0055\left(\frac{\varsigma(v_b t)-s}{b\,sen\left(\frac{\pi\tau}{180}\right)}+0{,}3\right)^{5/2}}{\mathrm{Fr}^2}\right] \tag{12}$$

This expression introduces a nonlinear effect into equations (2). In order to obtain analytical closed form results, a simple linearization is introduced interpolating the lift force through a straight line passing through the origin of the axes and for the extreme point $L_{Skid}(\Delta = \Delta_{MAX})$.

$$L_{Skid} = \frac{L_{Skid}(\Delta=\Delta_{MAX})}{\Delta_{MAX}}\Delta = \mu\,(\varsigma(v_b t) - s) \tag{13}$$

where $\mu = \frac{L_{Skid}(\Delta=\Delta_{MAX})}{\Delta_{MAX}}$:

$$\mu = \frac{1}{2}\rho {v_b}^2 \frac{1}{sin\left(\frac{\pi\tau}{180}\right)} b\;\; \tau^{1{,}1}\left[0.024 + \frac{0.176}{\frac{{v_b}^2}{gb}}\right] \tag{14}$$

Thus, the linear system is obtained:

$$\begin{cases} \ddot{z}m_b - c\dot{s} + c\dot{z} - ks + kz = 0 \\ \ddot{s}m_s - c\dot{z} + c\dot{s} - kz + (k+\mu)s = \mu\,\varsigma(v_b t) \end{cases} \tag{15}$$

In matrix form

$$\begin{bmatrix} m_b & 0 \\ 0 & m_s \end{bmatrix}\begin{pmatrix} \ddot{z} \\ \ddot{s} \end{pmatrix} + \begin{bmatrix} \mathrm{c} & -\mathrm{c} \\ -\mathrm{c} & \mathrm{c} \end{bmatrix}\begin{pmatrix} \dot{z} \\ \dot{s} \end{pmatrix} + \begin{bmatrix} k & -k \\ -k & k+\mu \end{bmatrix}\begin{pmatrix} \mathrm{z} \\ \mathrm{s} \end{pmatrix} = \begin{pmatrix} 0 \\ \mu\,\varsigma(v_b t) \end{pmatrix} \tag{16}$$

$$\mathbf{M}\ddot{\mathbf{z}}(t) + \mathbf{C}\dot{\mathbf{z}}(t) + \mathbf{K}\mathbf{z}(t) = \mathbf{F}(t) \tag{17}$$

3. ENCOUNTERED WAVE SPECTRUM RESPONSE

The force $\boldsymbol{F}(t)$ has stochastic nature depending on the wave profile $\varsigma(v_b t)$ met by the ship at a given speed v_b. The system response is studied through the spectral density of $\boldsymbol{z}$ and the spectral density of sea wave elevation is needed. Several theoretical energy spectra are available in the technical literature. In this case the Pierson-Moskowits spectrum is used:

$$S_{Sea}(\omega) = \frac{\alpha g^2}{\omega^5} e^{-\beta\left(\frac{g}{v_{W_{19.5}}\omega}\right)^4} \tag{18}$$

with $v_{w_{19.5}}$ the wind speed in m/s calculated at a standard height of $19.5m$ above the sea level, $\alpha = 0.0081$ and $\beta = 0.74$. The variance of the wave height follows:

$$\sigma^2_{\varsigma(t)} = \int_0^\infty S_{Sea}(\omega)d\omega = 2.74 \cdot 10^{-3} \frac{{v_{W_{19.5}}}^4}{g^2} \tag{19}$$

$S_{Sea}(\omega)$ represents the sea spectrum when the boat is at rest. In general, the sea wave elevation can be determined by a superposition of traveling waves as:

$$\varsigma(\mathrm{x,t}) = \sum_{n=0}^{+\infty} A_n \sin(\kappa_n x \pm \omega_n t + \varphi_n) \tag{20}$$

where the individual amplitudes are random variables and are determined from the power spectral density as $A_n = \sqrt{2S_{Sea}(\omega_n)\Delta\omega}$, where $\omega_n = 2\pi f_n$ are the frequency components of the signal, to which are associated the wavenumbers $\kappa_n = \frac{2\pi}{L_n}$ and the random phases φ_n. In general, κ and ω are related by the Airy's wave dispersion relationship $\omega^2 = g\kappa\tanh(\kappa d)$, with d the water depth. For $d \gg L$ or in the presence of deep water, than $\kappa d \gg 1$, and $\tanh(\kappa d) \cong 1$. Approximating the dispersion relation as $\omega^2 = g\kappa$, then the phase velocity becomes $c = \frac{\omega}{k} = \frac{g}{\omega}$. Substitution of the previous expressions into equation (20) ($\kappa_n = \frac{{\omega_n}^2}{g}$) produces:

$$\varsigma(\mathrm{x,t}) = \sum_{n=0}^{+\infty} \sqrt{2S_{Sea}(\omega_n)\Delta\omega}\sin\left(\frac{{\omega_n}^2}{g}x \pm \omega_n t + \varphi_n\right) \tag{21}$$

that completely solves the problem of describing the space-time wave elevation on the basis of the sea spectrum $S_{Sea}(\omega)$. However, the spectrum involved in equation (15) asks for the wave elevation experienced by the skid when travelling at the speed v_b. Thus, the Pierson-Moskowitz spectrum $S_{Sea}(\omega)$ must be suitably modified to take into account the boat motion. Moreover, the location x appearing in (21) is in this case intrinsically time-dependent, because of the relationship $x = v_b t$. Thus:

$$\varsigma(\mathrm{t},v_b) = \sum_{n=0}^{+\infty} \sqrt{2S_{Sea}(\omega_n)\Delta\omega}\sin\left(\left(\frac{{\omega_n}^2}{g}v_b \pm \omega_n\right)t + \varphi_n\right) \tag{22}$$

With $\widehat{\omega}_n = \left(\frac{{\omega_n}^2}{g}v_b \pm \omega_n\right)$, the expression modifies as:

$$\varsigma(\mathrm{t},v_b) = \sum_{n=0}^{+\infty} \sqrt{2S_{Sea}(\omega_n)\Delta\omega}\sin(\widehat{\omega}_n t + \varphi_n) \tag{23}$$

Finally the spectrum $\hat{S}_{Sea}(\widehat{\omega}, v_b)$ perceived by the skid undergoes a frequency shifting due to the skid speed, but still maintains its energy content, thus $\hat{S}_{Sea}(\widehat{\omega}, v_b)\Delta\widehat{\omega} = S_{Sea}(\omega_n)\Delta\omega$, where $\omega_n = \frac{-1+\sqrt{1+4\frac{v_b}{g}\widehat{\omega}_n}}{\frac{2v_b}{g}}$. Therefore:

$$\hat{S}_{Sea}(\hat{\omega}, v_b) = \frac{1}{\left(\frac{2\left(\frac{-1+\sqrt{1+4\frac{v_b}{g}\hat{\omega}_n}}{\frac{2v_b}{g}}\right)}{g}v_b+1\right)} \frac{\alpha g^2}{\left(\frac{-1+\sqrt{1+4\frac{v_b}{g}\hat{\omega}_n}}{\frac{2v_b}{g}}\right)^5} e^{-\beta\left(\frac{g}{v_{w_{19.5}}\left(\frac{-1+\sqrt{1+4\frac{v_b}{g}\hat{\omega}_n}}{\frac{2v_b}{g}}\right)}\right)^4} \tag{24}$$

3.1 Standard deviation of the heave motion of the skid

The linearized equations of motion in the frequency domain are:

$$[-\hat{\omega}^2\boldsymbol{M} + i\hat{\omega}\mathbf{C} + \boldsymbol{K}]\boldsymbol{Z}(\hat{\omega}) = \boldsymbol{F}(\hat{\omega}) \tag{25}$$

The transfer matrix is:

$$\boldsymbol{H}(i\hat{\omega}) = [-\hat{\omega}^2\boldsymbol{M} + i\hat{\omega}\mathbf{C} + \boldsymbol{K}]^{-1} \tag{26}$$

The power spectral response of the hull-skid system follows as:

$$\boldsymbol{S_Z}(\hat{\omega}) = \boldsymbol{H}(i\hat{\omega})^*\boldsymbol{S_F}(\hat{\omega})\boldsymbol{H}(i\hat{\omega}) \tag{27}$$

$$\begin{bmatrix} S_{zz}(\hat{\omega}) & S_{zs}(\hat{\omega}) \\ S_{sz}(\hat{\omega}) & S_{ss}(\hat{\omega}) \end{bmatrix} = \begin{bmatrix} H_{11}(i\hat{\omega})^* & H_{12}(i\hat{\omega})^* \\ H_{21}(i\hat{\omega})^* & H_{22}(i\hat{\omega})^* \end{bmatrix} \begin{bmatrix} 0 & 0 \\ 0 & \mu\hat{S}_{Sea}(\hat{\omega}, v_b) \end{bmatrix} \begin{bmatrix} H_{11}(i\hat{\omega}) & H_{12}(i\hat{\omega}) \\ H_{21}(i\hat{\omega}) & H_{22}(i\hat{\omega}) \end{bmatrix} \tag{28}$$

$$S_{ss}(\hat{\omega}) = H_{22}(i\hat{\omega})^*\mu\hat{S}_{Sea}(\hat{\omega}, v_b)H_{22}(i\hat{\omega}) \tag{29}$$

$$S_{ss}(\hat{\omega}) = |H_{22}(i\hat{\omega})|^2\mu\hat{S}_{Sea}(\hat{\omega}, v_b) \tag{30}$$

Then, the variance of the skid heave response is:

$$\sigma_s^2 = \int_0^\infty S_{ss}(\hat{\omega})d\hat{\omega} \tag{31}$$

$$\sigma_s^2 = \int_0^\infty |H_{22}(i\hat{\omega})|^2\mu\hat{S}_{Sea}(\hat{\omega}, v_b)\, d\hat{\omega} \tag{32}$$

The depth of the skid trailing edge can be statistically estimated as:

$$\Delta = -\sigma_{\varsigma(t)} - \sigma_s + \left|\Delta_{eq}\right| \tag{33}$$

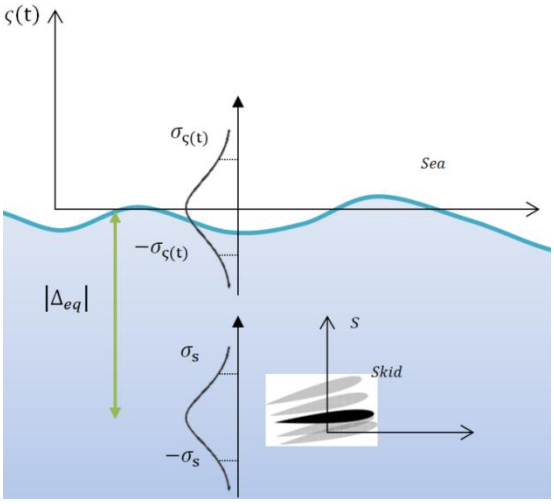

Figure 5: Diagram of the results obtained

If Δ is positive, the skid is submerged and it maintains a continuous contact with the water; if Δ is negative, the occurrence of skid water exits is expected and a skid-water intermittent contact is predicted.

4. RESULTS AND CONCLUSIONS

The use of the previous equations, permits to determine, given the sea state characterized by the wind speed, to increase the boat speed until $\Delta = 0$: the boat speed at which the depth vanishes is called the critical speed associated to the given wind speed. Modifying the wind speed we obtain different values for the critical boat speed. The pairs wind-speed and boat-speed describe a curve in the boat-speed wind-speed plane as it appears in Figure 6, named critical curve, the bound separating two navigation conditions: the continuous contact and the intermittent contact regions.

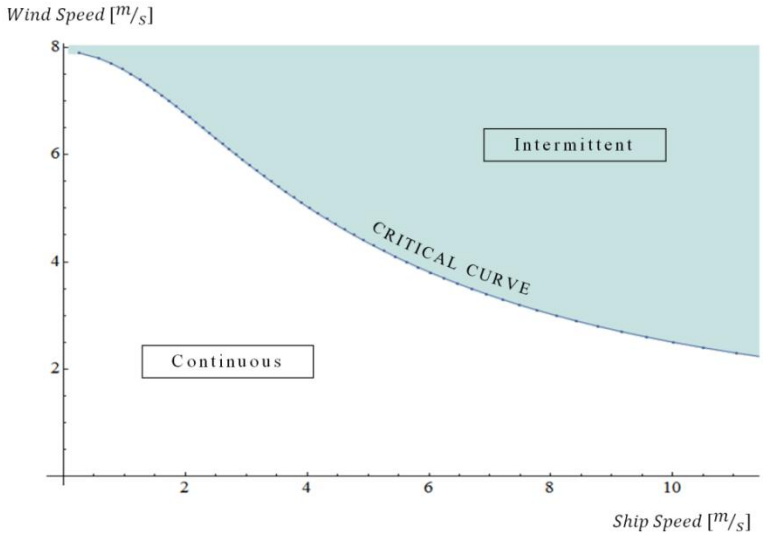

Figure 6: Critical curve with $\tau = 14°$, $m_b = 50kg$, $m_s = 1{,}5kg$.

Of course, changing the system parameters, the curve also changes. In Figure 7, for example, different boat displacements are considered, while in Figure 8 the skid angle of attack has been modified.

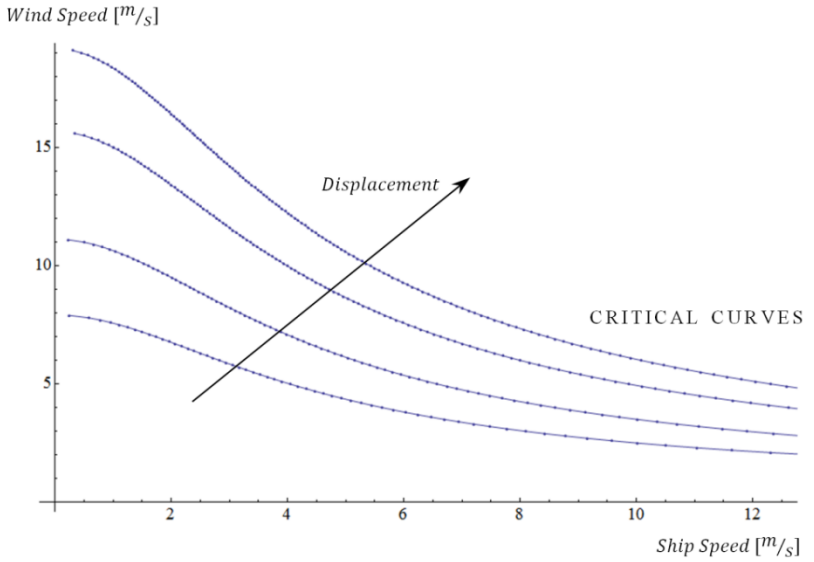

Figure 7: Critical curve with $\tau = 14°$, $m_b = [50 - 300]kg$, $m_s = 1{,}5kg$.

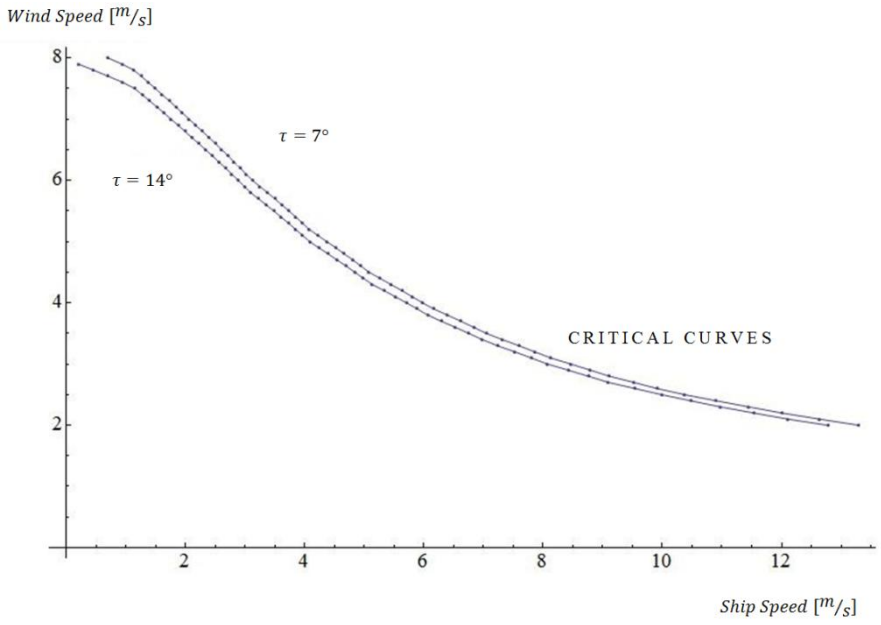

Figure 8: Critical curve with $\tau = [7° - 14°]$, $m_b = 50kg$, $m_s = 1{,}5kg$.

Figure 9 shows the three-dimensional plot to determine the critical curve.

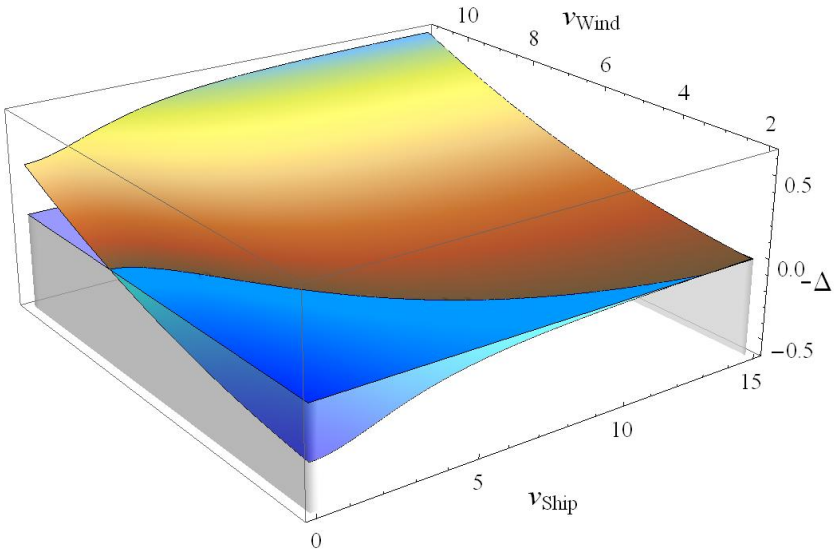

Figure 9: Three-dimensional plot of the critical curve for $\tau = 14°$, $m_b = 50kg$, $m_s = 1{,}5kg$, in blue the continuous contact region.

From the previous analysis it can be concluded that: (i) when a ship is equipped with a suspension skid, two different navigation conditions can be determined: the continuous contact region and the intermittent contact region, separated by the critical curve (depending on the ship speed and by the sea state); (ii) the intermittent contact for the skid motion, can produce several benefits because it activates the vehicle jumps, mitigating the severity of the heave response, that becomes largely independent of the wave shape and also reducing the average drag of the vehicle; (iii) the jumping navigation is allowed only by the installation of a suspension system that alleviates the severity of the water re-entry shocks.

REFERENCES

Carcaterra, A., & Ciappi, E. (2000). Prediction of the Compressible Stage Slamming Force on Rigid and Elastic System Impacting over the Water Surface. *Nonlinear Dynamics, 2*(21), 193-220.

Carcaterra, A., & Ciappi, E. (2004). Hydrodynamic shock of elastic structures impacting on the water: theory and experiments. *Journal of Sound and Vibration*(271), 411-439.

Carcaterra, A., Ciappi, E., Iafrati, A., & Campana, E. F. (2000). Shock Spectral Analysis of Elastic Systems Impacting on the Water Surface. *Journal of Sound and Vibration, 3*(229), 579-605.

Carcaterra, A., Dessi, D., & Mastroddi, F. (2005). Hydrofoil vibration induced by a random flow: a stochastic perturbation approach. *Journal of Sound and Vibration*(283), 401-432.

Carcaterra, A., Scorrano, A., & Pepe, G. (2011). SEALAB: Aero-hydro mechanics of a three-wings jumping vehicle. *HSMV2011*.

Carcaterra, A., Scorrano, A., Pepe, G., & Sestieri, A. (2011). SEALAB: Aero-hydro mechanics of an extreme-speed marine vehicle. *AIMETA2011*.

Collu, M., Patel, M. H., & Trarieux, F. (2007). A Unified Mathematical Model for High Speed Hybrid (Air and Water-borne) Vehicles. *Second Int. Conf. on Marine Research and Transportation*.

Dessi, D., & Mariani, R. (2008). Analysis and prediction of slamming-induced loads of a high-speed monohull in regular waves. *Journal of Ship Research, 1*(52).

Faltinsen, O. M. (2006). *Hydrodynamics of high speed marine vehicles.* Cambridge University Press.

Fossen, T. I. (1994). *Guidance and Control of Ocean Vehicles.* New York: John Wiley & Sons.

Pepe, G., Carcaterra, A., Scorrano, A., & Sestieri, A. (2011). Stability analysis of a three-wings high-speed craft. *AIMETA2011*.

Peri, D., & Campana, E. F. (2003). Multidisciplinary Design Optimization of a Naval Surface Combatant. *Journal of Ship Research, 1*(47).

Pinto, A., Peri, D., & Campana, E. F. (2004). Global optimization algorithms in naval hydrodynamics. *Ship Technology Research, 3*(51).

Savitsky, D. (1964). Hydrodinamic Design of Planing Hulls. *Marine Technology, Vol.1*(No. 1), pp. 71-95.